

Highly tunable SrTiO₃/DyScO₃ heterostructures for applications in the terahertz range

P. Kužel,^{a)} F. Kadlec, and J. Petzelt

Institute of Physics, Academy of Sciences of the Czech Republic, Na Slovance 2, 182 21 Prague 8, Czech Republic

J. Schubert and G. Panaitov

Institute of Bio- and Nano-Systems and Center of Nanoelectronics and Information Technology (CNI), Forschungszentrum Jülich GmbH, D 52425 Jülich, Germany

(Received 2 November 2007; accepted 16 November 2007; published online 7 December 2007)

Several types of multilayer structures based on SrTiO₃ and DyScO₃ thin films were prepared by laser ablation. The dielectric properties of these samples without and under applied static or low-frequency electric field at room temperature were determined in the terahertz spectral range by time-domain terahertz spectroscopy. We demonstrate up to 65% variation of the permittivity of SrTiO₃ films and up to 33% modulation of the power transmission of terahertz waves at 500 GHz and 100 V (67 kV/cm) bias. © 2007 American Institute of Physics. [DOI: 10.1063/1.2822409]

The optical or electrical control of the propagation of terahertz radiation is of high importance in the current terahertz technology and has recently received considerable attention.¹⁻³ Ferroelectric materials are suitable for the modulation of the real part of the permittivity by applied bias or temperature.⁴ Strontium titanate [(SrTiO₃) (STO)] is an incipient ferroelectric material. Its dielectric behavior is fully controlled by the soft mode which exhibits a frequency decrease upon cooling, while the material remains paraelectric down to the lowest temperatures due to quantum fluctuations.⁵ This leads to an increase of the permittivity of STO and of its tunability with decreasing temperature.

Strain is one of the important factors affecting the ferroelectric properties of STO because of its strong coupling to the polarization. It is possible to prepare epitaxial thin STO films on different substrates with the aim to finely tune the lattice mismatch between STO and the substrate material and the strain within the film, namely, a ferroelectric phase transition can be induced in STO thin films by a tensile strain.^{6,7} The transition temperature can be increased by a suitable substrate choice and the material can be made more suitable for room temperature applications.

The properties of STO grown on DyScO₃ (DSO) substrates have been extensively studied during the last years.⁶⁻¹¹ In this letter, we report on the terahertz dielectric properties and tunability of STO/DSO multilayer structures deposited on DSO substrates. We compare the results with those previously obtained with a 300 nm STO film deposited on a sapphire substrate (sample STO-s).³

The STO thin film structures were prepared by pulsed laser deposition on (110)-oriented 10 × 10 × 0.9 mm³ DSO substrates in an on-axis geometry using a KrF laser ($\lambda=248$ nm, pulse width 25 ns, and a fluence of 2.5 J/cm²).¹² The targets were a single crystal of STO and a DSO polycrystal.¹³ The substrates were positioned directly onto a SiC resistive heater, and an O₂ partial pressure of 0.2 Pa was used. An interdigitated gold electrode structure was deposited onto the multilayers so that it covered about half of

the sample surface. It was prepared by lift-off photolithography using 20 nm Nb/300-nm-thick Au films deposited by dc magnetron sputtering. The 6 × 6 mm² interdigitated structure consisted of 5 μ m wide gold lines and 15 μ m wide gaps.³ The electrode fingers were parallel to the [101] direction of the DSO substrate (notation of Ref. 7). The electrodes act as a polarizer with a high transmittance for the terahertz electric field $E_{\text{THz}} \parallel [010]$. The experiments were made under normal incidence, i.e., the wave vector of the terahertz radiation was parallel to the [10 $\bar{1}$] direction of the DSO substrate. Four samples were prepared.

- First is a single bare 100-nm-thick STO layer (sample 1 × 100A). The substrate temperature during the deposition was about 40 °C higher than for the other samples.
- Second is a single 100-nm-thick STO with the electrodes deposited on top (sample 1 × 100B).
- Third is a multilayer with the electrodes consisting of four STO/DSO bilayers where the thickness of each layer was 50 nm, i.e., the total thickness of STO was 200 nm (sample 4 × 50).
- Fourth is a multilayer with the electrodes consisting of 20 STO/DSO bilayers where the thickness of each layer was 10 nm, i.e., with the total STO thickness of 200 nm (sample 20 × 10).

For the terahertz time-domain experiments, we used a Ti:sapphire femtosecond laser oscillator. Linearly polarized terahertz probing pulses were generated using an interdigitated photoconducting switch¹⁴ and detected using the usual electro-optic sampling scheme with a 1-mm-thick [110] ZnTe crystal.¹⁵

In a first series of experiments we have determined the complex permittivity spectra of the STO layers without bias; for this purpose we used the parts of the samples without electrodes. The experiments consisted of two consecutive measurements: that of a waveform $E_s(t)$ by using a sample with the thin film structure and another one of a reference waveform $E_r(t)$ with a bare DSO substrate. The ratio of the

^{a)} Author to whom correspondence should be addressed. Electronic mail: kuzelp@fzu.cz.

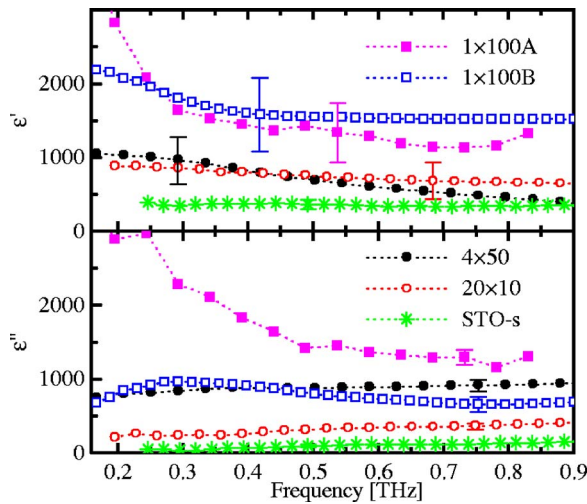


FIG. 1. (Color online) Zero-field permittivity and losses of STO films.

respective Fourier transforms provides the complex terahertz transmittance spectrum of the film: $t(\omega) = E_s(\omega) / E_i(\omega)$.

The evaluation of the dielectric response of STO was made under the assumption of a uniformly strained STO, i.e., that all the STO layers of the structure are homogenous and described by the same dielectric function $\varepsilon = \varepsilon' + i\varepsilon''$. However, it is likely that a depth gradient of the strain and dielectric response does exist; this effect then may appear as inhomogeneous broadening in the resulting dielectric spectra.

The optical thickness of any film within the multilayers ($\leq 3 \mu\text{m}$) is much smaller than the wavelength of the terahertz radiation ($> 150 \mu\text{m}$). It can be easily shown (e.g., using the transfer matrix formalism¹⁶) that the terahertz transmission through an STO/DSO multilayer is equivalent to that through an STO/DSO bilayer with the same overall thickness of each material (i.e., a 200-nm-thick STO layer plus a 200-nm-thick DSO layer in the case of our 4×50 and 20×10 samples). The refractive index of the STO films $N = \varepsilon^{1/2}$ is then determined by inverting the expression¹⁷

$$t(\omega) = \frac{2N(N_s + 1) \exp\{i\omega[(N-1)d + (N_s-1)(d_s - d_r)]/c\}}{(1+N)(N+N_s) + (1-N)(N-N_s) \exp[2i\omega Nd/c]}, \quad (1)$$

where d is the total thickness of STO layers, N_s is the complex refractive index of DSO, d_s is the substrate thickness, d_r is the thickness of the reference sample (bare DSO substrate), and c is the speed of light in vacuum.

Results of the measurements are shown in Fig. 1. We found no substantial difference between the polarizations $E_{\text{THz}} \parallel [101]$ and $E_{\text{THz}} \parallel [010]$. The error bars are related mainly to the uncertainty in d_s and d_r , as discussed in Ref. 17. Note a clear increase in the permittivity (ε') and losses (ε'') of the 20×10 sample as compared to STO-s.³ A further increase of ε'' is observed for the 4×50 structure (while ε' remains close to 1000). The $1 \times 100\text{B}$ structure containing a single STO film exhibits an additional increase in ε' while ε'' stays at the level of the 4×50 sample. All these samples display an increasing (or constant) ε'' and slightly decreasing ε' with frequency. This gives evidence of a strong influence of the (heavily damped) soft mode in this part of the spectrum.³ The high damping of the soft mode can be attributed to the inhomogeneous distribution of the strain in the structure. For a more specific assignment a higher frequency

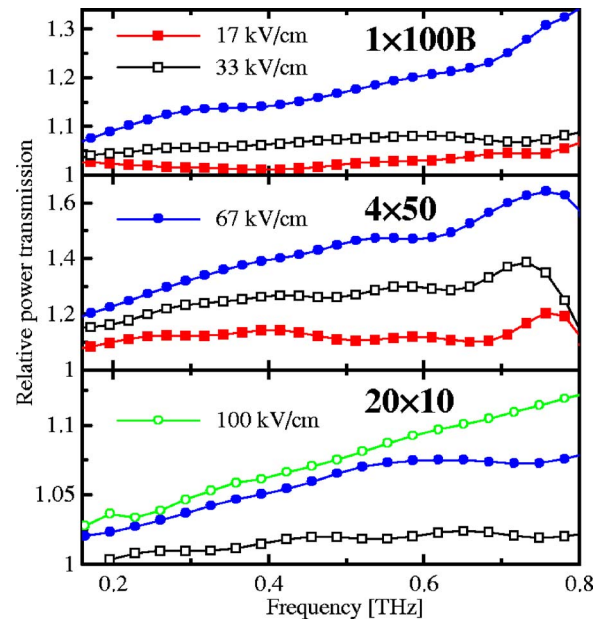


FIG. 2. (Color online) Power transmission spectra of the investigated samples. We plot here the ratio between the terahertz transmittances with and without bias: $|E_V/E_0|^2$.

response and temperature dependences should be determined (corresponding measurements are in progress). The above described spectra are in a strong contrast with the behavior observed for the sample $1 \times 100\text{A}$, where a low-frequency contribution (central peak) clearly dominates and is at the origin of a high dispersion below 500 GHz. The central peak presumably exists even in the other strained samples, however, its role is much smaller. This might be related to the film growth processing, as indicated by the recently reported strong influence of annealing of STO films on the permittivity in the gigahertz range;⁸ in that case the 10 GHz permittivity of annealed samples was significantly reduced. The central peak can be related to the contribution of ferroelectric domain walls and/or polar clusters in the strain-induced ferroelectric phase which is known to show relaxor behavior.^{10,11} Evidence of the central mode contribution to the permittivity in the 10–100 GHz range close to ferroelectric transition temperatures was recently obtained also from bulk (Ba,Sr)TiO₃ ceramics¹⁸ and seems to be a general phenomenon near displacive ferroelectric transitions.¹⁹

In a second series of experiments we characterized the electric field dependence of the terahertz dielectric response of the samples: a dc bias was applied to the samples and transmission spectra were measured with $E_{\text{THz}} \parallel [010]$. We verified that the same results are obtained if a low-frequency bias field at 166 Hz is used. In Fig. 2 we show the power transmission spectra of the biased samples normalized to the zero-field spectra. They show the possibility of using some of the investigated structures as terahertz modulators: a ratio of nearly 1.5 (33% transmission modulation) is obtained at 0.5 THz with the sample 4×50 for an applied voltage of 100 V (67 kV/cm). This behavior is related to a strong electric field dependence of both real and imaginary parts of the permittivity.

The dielectric function of the films under external field $\varepsilon(V)$ was calculated from the spectra of the terahertz pulses transmitted through the biased samples and we used here the pulses transmitted through the unbiased samples as refer-

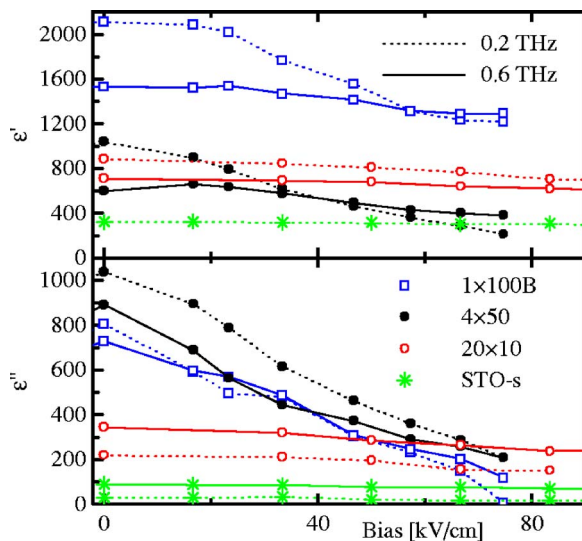


FIG. 3. (Color online) Real and imaginary parts of the dielectric function of STO films as a function of external electric field.

ence. Figure 3 shows the dependence of the complex permittivity at 0.2 and 0.6 THz upon the applied field and Fig. 4 displays the modulation of the permittivity versus frequency for high and moderate values of the field. The prominent features observed in these plots are: (1) The permittivity ϵ' exhibits a roughly quadratic decrease with the applied field for all samples; this decrease is quite high for $1 \times 100\text{B}$ (nearly by a factor of 2) and 4×50 (by a factor of 3) samples at the highest fields at 0.2 THz. (2) The losses ϵ'' show a steep approximately linear drop even for a low bias; again, the samples with high losses without field ($1 \times 100\text{B}$ and 4×50) are characterized by the fastest decrease and, at high fields, ϵ'' reaches values comparable to those of the unstrained sample. (3) The high negative change in ϵ' at low frequencies (Fig. 4) suggests an important role of the broad central mode. Together with the steep linear drop of ϵ'' displayed in Fig. 3, it indicates that the central mode is probably

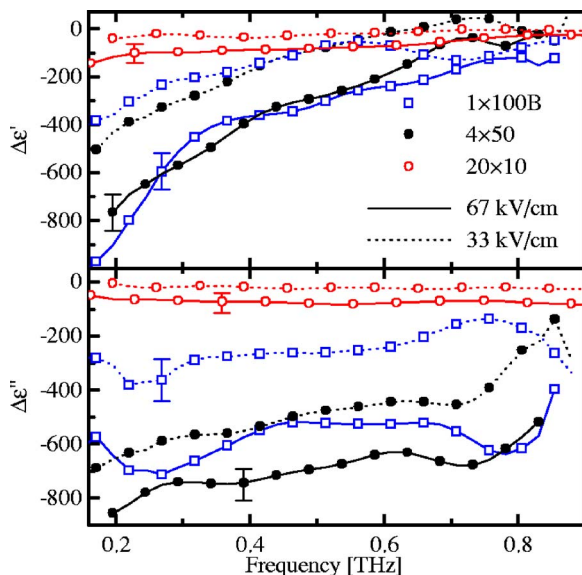


FIG. 4. (Color online) Electric field induced modulation of the permittivity and losses $\Delta\epsilon = \epsilon(V) - \epsilon(0)$ of STO films for two values of the external electric field.

very sensitive to external parameters (growth conditions, field, strain, etc) and rapidly vanishes when the field is applied. This could mean that the central peak is due to the contribution of domain walls or polar clusters which is strongly influenced by the bias.^{10,11} (4) The tunabilities of $1 \times 100\text{B}$ and 4×50 samples are similar; however, the overall thickness of STO in the latter one is twice as high as in the former one. This yields a higher figure of merit of the latter sample for the terahertz transmission modulation, as shown in Fig. 2.

To summarize, we characterized the dielectric properties of strained STO thin films in several multilayer structures grown on DSO substrates in the terahertz range. The soft mode is heavily damped in strained samples and a central mode plays an important role in the subterahertz range. Strained samples show a significant enhancement of the tunability of both permittivity and losses; the highest influence of applied bias was found in the multilayer with intermediate thickness of layers (50 nm). The multilayer samples show also a potential for applications as terahertz modulators.

The authors thank N. Klein for helpful discussions. This work was supported by the Ministry of Education of the Czech Republic (Project No. LC-512), by the Czech Academy of Sciences (Project No. AVOZ 10100520) and by an exchange program between DAAD and ASCR (D20-CZ 4/06-07).

¹H.-T. Chen, W. J. Padilla, J. M. O. Zide, A. C. Gossard, A. J. Taylor, and R. D. Averitt, *Nature (London)* **444**, 597 (2006).

²L. Fekete, F. Kadlec, H. Němec, and P. Kužel, *Opt. Express* **15**, 8898 (2007).

³P. Kužel, F. Kadlec, H. Němec, R. Ott, E. Hollmann, and N. Klein, *Appl. Phys. Lett.* **88**, 102901 (2006).

⁴A. K. Tagantsev, V. O. Sherman, K. F. Astafiev, J. Venkatesh, and N. Setter, *J. Electroceram.* **11**, 5 (2003).

⁵K. A. Müller and H. Burkard, *Phys. Rev. B* **19**, 3593 (1979).

⁶J. H. Haeni, P. Irvin, W. Chang, R. Uecker, P. Reiche, Y. L. Li, S. Choudhury, W. Tian, M. E. Hawley, B. Craigo, A. K. Tagantsev, X. Q. Pan, S. K. Streiffer, L. Q. Chen, S. W. Kirchoefer, J. Levy, and D. G. Schlom, *Nature (London)* **430**, 758 (2004).

⁷R. Wördenweber, E. Hollmann, R. Kutzner, and J. Schubert, *J. Appl. Phys.* **102**, 044119 (2007).

⁸W. Chang, J. A. Bellotti, S. W. Kirchoefer, and J. M. Pond, *J. Electroceram.* **17**, 487 (2006).

⁹M. Boese, T. Heeg, J. Schubert, and M. Luysberg, *J. Mater. Sci.* **41**, 4434 (2006).

¹⁰P. Irvin, J. Levy, J. H. Haeni, and D. G. Schlom, *Appl. Phys. Lett.* **88**, 042902 (2006).

¹¹A. Vasudevarao, A. Kumar, L. Tian, J. H. Haeni, Y. L. Li, C.-J. Eklund, Q. X. Jia, R. Uecker, P. Reiche, K. M. Rabe, L. Q. Chen, D. G. Schlom, and V. Gopalan, *Phys. Rev. Lett.* **97**, 257602 (2006).

¹²L. Beckers, J. Schubert, W. Zander, J. Ziesmann, A. Eckau, P. Leinenbach, and C. Buchal, *J. Appl. Phys.* **83**, 3305 (1998).

¹³T. Heeg, J. Schubert, Ch. Buchal, E. Cicerella, J. L. Freeouf, W. Tian, Y. Jia, and D. G. Schlom, *Appl. Phys. A: Mater. Sci. Process.* **83**, 103 (2006).

¹⁴A. Dreyhaupt, S. Winnerl, T. Dekorsy, and M. Helm, *Appl. Phys. Lett.* **86**, 121114 (2005).

¹⁵A. Nahata, A. S. Welington, and T. F. Heinz, *Appl. Phys. Lett.* **69**, 2321 (1996).

¹⁶M. Born and E. Wolf, *Principles of Optics*, 7th ed. (Cambridge University Press, New York, 2003).

¹⁷J. Petzelt, P. Kužel, I. Rychetský, A. Pashkin, and T. Ostapchuk, *Ferroelectrics* **288**, 169 (2003).

¹⁸T. Ostapchuk, M. Savinov, J. Petzelt, A. Pashkin, M. Dressel, E. Smirnova, V. Lemanov, A. Sotnikov, and M. Weihnacht, *Ferroelectrics* **353**, 70 (2007).

¹⁹E. Buixaderas, S. Kamba, and J. Petzelt, *Ferroelectrics* **308**, 131 (2004).